A Metal-free Porphyrin Heterogenised onto SBA-15 Silica: a Performant Material for the CO_2 Cycloaddition to Epoxides and Aziridines

Paolo Sonzini,[a] Nicolas Berthet,[b] Caterina Damiano,[a] Véronique Dufaud[b]* and Emma Gallo[a]*

[a]*Department of Chemistry, University of Milan, Via Golgi, 19, I-20133 Milan, Italy; E-mail: emma.gallo@unimi.it*

[b]*University of Lyon, CPE Lyon, CNRS, UMR 5128, Catalysis, Polymerization, processes and Materials (CP2M), 43 Bd du 11 novembre 1918, F-69616 Villeurbanne cedex, France; E-mail: veronique.dufaud@univ-lyon1.fr*

Abstract. The covalently heterogenisation of a free-base porphyrin on SBA-15 silica yielded **TPPH$_2$@SBA-15** (**TPPH$_2$** = tetraphenyl porphyrin), which was very efficient to promote the CO_2 cycloaddition to three-membered rings. The **TPPH$_2$@SBA-15**/TBAX-based catalytic procedure was very general, as revealed by excellent activities registered in the reaction of CO_2 with epoxides, *N*-alkyl and *N*-aryl aziridines, forming cyclic carbonates, *N*-alkyl and *N*-aryl oxazolidinones, respectively. It is worth noting that this is the first example of the heterogeneously catalysed synthesis of *N*-aryl oxazolidinones from corresponding *N*-aryl aziridines. The scale-up of the methodology highlighted that catalytic performances of all the three investigated reactions were maintained also working at a gram-scale to pave the way for future developments of the procedure. In addition, the recycle of **TPPH$_2$@SBA-15** for several consecutive reactions was efficient and observed catalytic activities were very similar to those registered in the presence of a fresh material. All the acquired data indicated an excellent sustainability of the catalytic protocol to envisage upcoming practical applications.

Keywords: Carbon Dioxide, Epoxide, Aziridine, Cycloaddition, Heterogenised porphyrin

1. Introduction

The atmospheric concentration of carbon dioxide, the most abundant greenhouse gas, has reached its highest level ever due to human activities, exceeding the fateful threshold of 400 ppm with dramatic consequences on global warming and human health [1]. Besides CO_2 capture and storage technologies developed so far [2-4], the use of carbon dioxide as a renewable and inexpensive raw starting material in organic transformations appears particularly attractive as it could lead to the reduction of the carbon footprint of new chemicals and our dependence on fossil

resources [5-10]. Considering that a large practical use of CO_2 as a C1 source in chemical synthesis has been hampered by its high stability (ΔH_f = -394 kJ.mol^{-1}), a great effort has been devoted to develop efficient catalytic systems capable of reducing the energy cost of CO_2 activation.

Among the synthetic methods currently available, the catalysed carbon dioxide cycloaddition to epoxides [11-13] and aziridines [14-19] is one of the most successful examples of eco-fixation of this waste thanks to the 100% atom economy of these processes with respect to traditional routes that use highly toxic reagents such as phosgene [20] (Scheme 1).

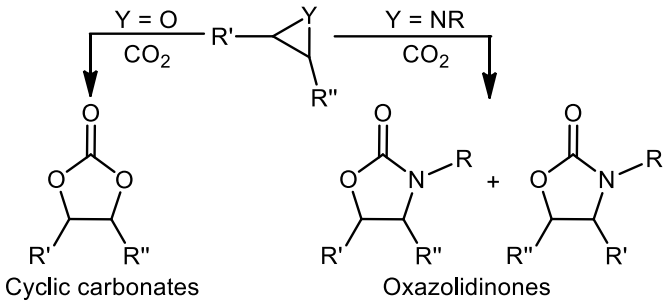

Scheme 1. General scheme of the CO_2 cycloaddition to epoxides and aziridines forming cyclic carbonates and oxazolidinones, respectively.

The importance of these synthetic procedures is related to the relevance of cyclic carbonates, which are used as polar aprotic solvents, lubricants, non-aqueous electrolytes, and monomers for polymers preparations [21-23], as well as of oxazolidinones that, besides being useful chiral auxiliaries in organic synthesis [24-25], present interesting pharmacological activities [26-27].

Complexes of N_2O_2-salen/salophen [28-30], N_4-ligands [31-32] and N_4-porphyrin ligands [33-34], metalated with Al, Co, Fe, Mg or Zn have been extensively used as Lewis acids (LA), in combination with ammonium salts (as Lewis bases, LB), to efficiently synthesise cyclic carbonates. However, in order to improve the process sustainability and avoid toxicity issues rising from the presence of metallic residues in the final products, transition metal-free mediated CO_2 fixation methodologies, including the use of phosphonium or imidazolium salts or metal-free salen and salophen ligands [12, 35], have recently attracted a great attention. Ammonium salts have been studied either alone [36] or in combination with organic molecules in order to improve catalytic performances [37-38]. Even if several metal-free catalytic protocols have been reported in literature, the moderate catalytic activity of these systems requires operating at high temperatures and pressures and consequently the design of more efficient systems that are active under milder experimental conditions remains a challenge.

Although *N*-alkyl aziridines are less reactive than epoxides with respect to CO_2, several synthetic protocols have been reported in literature [14-15, 39] by using transition metal-based catalytic

systems very similar to those reported for the synthesis of cyclic carbonate. Similarly to what reported above, also *N*-alkyl oxazolidin-2-ones can be synthesised by applying sustainable procedures, such as solvent-free [14] and metal free [40-43] homogeneous catalytic processes as well as heterogeneous catalytic procedures [18, 44].

While many papers have been published on the CO_2 cycloaddition to *N*-alkyl aziridines, the direct synthesis of *N*-aryl oxazolidin-2-ones from *N*-aryl aziridines [45-46] has been less investigated, in spite of the noticeable pharmaceutical activities of these 5-membered heterocycles [26, 47-49]. Additionally, to the best of our knowledge, the conversion of *N*-aryl aziridines into *N*-aryl oxazolidin-2-ones by using heterogeneous catalytic procedures has never been reported.

Recently, some of us reported on the use of the metal-free **TPPH$_2$**/TBACl binary system (**TPPH$_2$** = *meso*-tetraphenyl porphyrin; TBACl = tetrabutyl ammonium chloride) for the production of *N*-alkyl [50] and *N*-aryl [51] oxazolidin-2-ones by the direct coupling of CO_2 with *N*-aryl and *N*-alkyl aziridines, respectively. The presence of a transition metal coordinated into the tetrapyrrolic core, whose action is normally associated to the activation of the aziridine substrate, was not required to reach high catalytic performances. The beneficial role of **TPPH$_2$** to promote the overall reactivity was elucidated by DFT calculations and relates to the formation of a very stable **TPPH$_2$**/TBACl adduct, which was able of reducing the energy cost of the oxazolidine-2-one synthesis.

Based on what reported above, we here describe the synthesis, characterization and activity of the metal-free porphyrin-based material **TPPH$_2$@SBA-15** in promoting the cycloaddition of carbon dioxide to epoxides as well as *N*-alkyl and *N*-aryl aziridines, when used in combination with tetrabutyl ammonium salts. The optimisation of the reaction parameters and the study of the substrate scope of the heterogeneous catalytic CO_2 cycloaddition to both epoxides and aziridines are here presented and achieved results will be fundamental to pave the way to future applications in more sustainable procedures such as continuous-flow synthetic processes.

Conversely to what stated above on the synthesis of oxazolidinones mediated by free-base porphyrins, their use in promoting the formation of forming cyclic carbonates under homogeneous conditions has been rarely reported. To the best of our knowledge, the activity of $TPPH_2$ was tested only one time in the cycloaddition of CO_2 to 2-butyloxirane and compared to those of other macrocycles such as calix[4]pyrrole and calix[4]arene, which showed better performances due to the easier accessibility of the macrocyclic cavity of the organocatalyst [52].

Thus, in order to have a more general view of the activity of free-porphyrins and to better appreciate benefits of applying heterogeneous materials, a reaction scope of the synthesis of cyclic carbonates promoted by the soluble **TPPH$_2$**/TBACl binary catalytic system was fully investigated and here presented.

2. Experimental Section

2.1. Synthesis of N_3@SBA-15. Pluronic P123 (8.00 g, 1.37 mmol) was dissolved at 40 °C in 250.0 mL of a 2.00 M aqueous HCl solution. The solution was stirred till it became clear, then tetraethoxy-silane (16.77 g, 80.49 mmol) was added dropwise and the solution was stirred for 30 minutes prior the addition of 3-azidopropyltriethoxysilane (1.00 g, 3.99 mmol). The obtained mixture was kept 24 hours at 40 °C under stirring. The reaction mixture was then transferred into a steal autoclave and reacted at 100 °C for 24 hours. After cooling, the resulting solid was collected in a filter, washed with slightly acidic water and ethanol. The solid was dried at 60 °C for 15 hours and extracted by a Soxhlet using acetonitrile for 48 hours to remove Pluronic P123. Finally, the obtained white solid was dried at 80 °C in an oven for 12 hours.

2.2. Synthesis of $TPPH_2$@SBA-15. Triethylamine (0.607 g, 6.00 mmol) and **EtTPPZn** (Zn(5-(4-ethynylphenyl)-10,15,20-triphenylporphyrin) (0.34 g, 0.48 mmol) were added under argon atmosphere to a suspension of **N_3@SBA-15** (1.00 g, 0.24 mmol of azide) in dry toluene (30.0 ml). The reaction mixture was stirred for 30 minutes at room temperature before adding the copper iodide catalyst (0.23 g, 1.20 mmol) and then stirred at 25 °C for 4 days. The obtained purple powder was collected in a filter and washed 3 times with THF to separate the porphyrin excess. The powder was suspended in 40.0 mL of methanol, *N,N*-diethyldithiocarbamate sodium trihydrate (0.90 g, 3.99 mmol) was added and the resulting dark mixture was stirred for 2.0 hours. The obtained powder was collected in a filter and washed with methanol, THF and acetone. The solid was washed 5 times with HCl 0.5 M to remove the zinc from the porphyrin core. The obtained brown powder was washed with water, ethanol and acetone. The desired **$TPPH_2$@SBA-15** material was dried overnight at 80 °C in the oven.

2.3. General catalytic procedure for the synthesis of cyclic carbonates. The reactions were performed in a 2.0 mL glass liner equipped with a screw cap and glass wool that was placed into a stainless-steel autoclave and three vacuum-carbon dioxide cycles were performed. 0.6 MPa of CO_2 was charged at room temperature and the autoclave was heated to 150 °C and the reaction was stirred for 2.0 hours. Then, the autoclave was cooled to room temperature and slowly vented. The crude was analysed by ^{1}H NMR spectroscopy in the presence of 2,4-dibromomesitylene as the internal standard.

2.3.1. Under homogenous conditions. TBACl (0.29 mg, 1.12 x 10^{-6} mol), epoxide (2.18 x 10^{-3} mol) and **$TPPH_2$** (0.64 mg, 1.12 x 10^{-6} mol) were placed in a vessel. At the end of the reaction, the organic solvent was evaporated to dryness.

2.3.2. Under heterogeneous conditions. TBAI (0.41 mg, 1.12 x 10^{-6} mol, 0.05 mol% with respect to epoxide), epoxide (2.18 x 10^{-3} mol) and **TPPH$_2$@SBA-15** (0.05 mol% of anchored porphyrin with respect to epoxide) were placed in a vessel. At the end of the reaction, the silica was filtered off and washed three times with CH_2Cl_2 to recuperate the product. The organic solvent was evaporated to dryness.

2.4. General catalytic procedure for the synthesis of N-alkyl oxazolidinones.

The reactions were performed in a 2.0 mL glass liner equipped with a screw cap and glass wool that was placed into a stainless-steel autoclave and three vacuum-carbon dioxide cycles were performed. 0.6 MPa of CO_2 was charged at room temperature and the autoclave was heated to 150 °C and the reaction was stirred for 2.0 hours. Then, the autoclave was cooled to room temperature and slowly vented. The crude was analysed by ^{1}H NMR spectroscopy in the presence of 2,4-dibromomesitylene as the internal standard.

The reaction mixture was cooled to -78°C and the vessel was transferred into a stainless-steel autoclave. Three vacuum-nitrogen cycles were performed and 1.2 MPa CO_2 was charged at room temperature. The autoclave was placed in a preheated oil bath at 125°C and the reaction was stirred for 16.0 hours, then it was cooled to room temperature and slowly vented. The silica was filtered off and washed three times with CH_2Cl_2 to recover the product. The organic solvent was evaporated to dryness and the crude analysed by ^{1}H NMR spectroscopy in the presence of 2,4-dinitrotoluene as the internal standard.

2.4.1. Under heterogeneous conditions

TBAI (2 mol% with respect to aziridine) and **TPPH$_2$@SBA-15** (0.4 mol% of anchored porphyrin with respect to aziridine) were placed in a 2.0 mL glass liner equipped with a screw cap and glass wool, then, aziridine (9.38 x 10^{-4} mol) and 0.250 mL of dry THF were added. The reaction mixture was cooled to -78°C and the vessel was transferred into a stainless-steel autoclave. Three vacuum-nitrogen cycles were performed and 1.2 MPa CO_2 was charged at room temperature. The autoclave was placed in a preheated oil bath at 125°C and the reaction was stirred for 16.0 hours, then it was cooled to room temperature and slowly vented. The silica was filtered off and washed three times with CH_2Cl_2 to recover the product. The organic solvent was evaporated to dryness and the crude analysed by ^{1}H NMR spectroscopy in the presence of 2,4-dinitrotoluene as the internal standard.

2.6. General catalytic procedure for the synthesis of N-aryl oxazolidinones under heterogeneous conditions. TBACl (5 mol% with respect to aziridine) and **TPPH$_2$@SBA-15** (1.0 mol% of

anchored porphyrin with respect to aziridine) were placed in a 2.0 mL glass liner equipped with a screw cap and glass wool, then, the aziridine (3.75×10^{-4} mol) and 0.250 mL of dry THF were added. The reaction mixture was cooled to -78 °C and the vessel was transferred into a stainless-steel autoclave. Three vacuum-nitrogen cycles were performed and 1.2 MPa CO_2 was charged at room temperature. The autoclave was placed in a preheated oil bath at 125 °C and the reaction was stirred for 16.0 hours, then it was cooled to room temperature and slowly vented. The silica was filtered off and washed three times with CH_2Cl_2 to recover the product. The organic solvent was evaporated to dryness and the crude analysed by ^{1}H NMR spectroscopy in the presence of 2,4-dinitrotoluene as the internal standard.

3. Results and Discussion

3.1 Synthesis of metal-free porphyrin organic-inorganic hybrid material TPPH$_2$@SBA-15

In the design of organic-inorganic hybrid materials, the nature of the host matrix as well as its textural and structural properties are of crucial importance and can be effectively adapted to the guest size especially when large molecules such as porphyrins (the parent $TPPH_2$ molecules displays a porphyrin ring of approximately 1.0 nm) [53] are at stake. Periodic mesoporous silicas of the SBA families are particularly well suited for the immobilization of bulky relevant species due to their large surface areas (up to 1000 m^2/g), pore sizes ranging from 2 to 50 nm and tuneable ordered pore systems [54-56].

Among the different available methodologies, the covalent approach over non-covalent anchoring (i.e. adsorption, ion pair formation, entrapment) to tightly immobilise the porphyrin onto the silica surface was chosen. The strategy involved a two-steps procedure, as shown in Scheme 2. First, SBA-15 type silica was functionalised with azidopropyl groups by using a direct co-condensation approach, then a copper-catalysed azide/alkyne cycloaddition ("click" reaction) of **EtTPPZn** (5-(4-ethynylphenyl)-10,15,20-triphenylporphyrin, see SI) was performed to create robust triazole linkages. The one-pot co-condensation route to introduce the incipient azido tether was considered over post-grafting procedure as it provides for greater homogeneous distribution of functional groups within the solid.

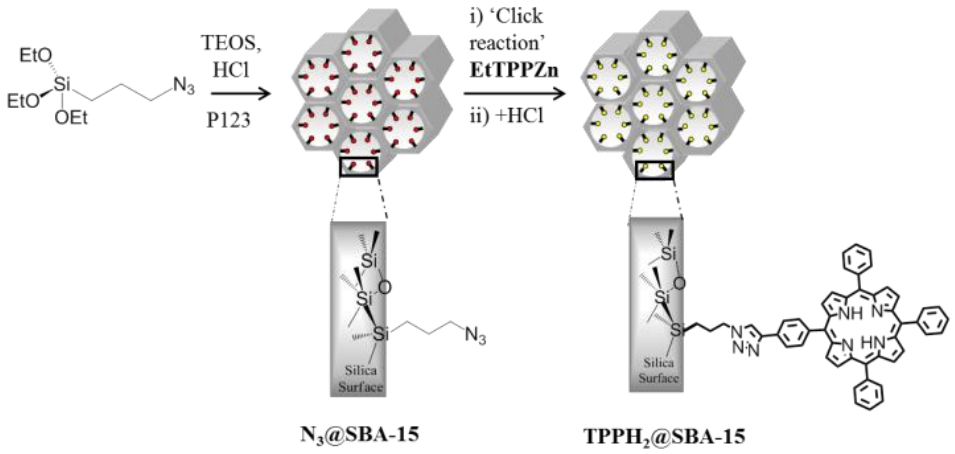

Scheme 2. Immobilization of **EtTPPH$_2$** through click chemistry.

To ensure the formation of discrete porphyrin species on the silica surface while maintaining a high concentration of silanol groups, which can also act as substrate activators through H-bonding (see below), an azidopropyl loading as low as 0.2 mmol.g^{-1} (corresponding to site isolation) was targeted. In order to avoid any competitive coordination of copper to the tetrapyrrolic core during the click reaction, zinc porphyrin was employed as the starting material and then the free-base porphyrin was re-established by washing with an acidic aqueous solution. The UV-Vis analyses (Figure S6, SI) showed that the linkage onto the silica was successfully performed and zinc was efficiently removed from the obtained solid. The comparison of the spectrum of the free porphyrin **TPPH$_2$** (Figure S6, left) with that of the **TPPH$_2$@SBA-15** hybrid-material (Figure S6, centre) evidenced in both cases the presence of the Soret band at 417 nm and the Q-bands between 500 and 650 nm, which are characteristic absorptions of metal-free porphyrins. The slight shift observed in the liquid UV-Vis spectrum, from 417 nm of **EtTPPH$_2$** to 424 nm of **TPPH$_2$@SBA-15**, could be due to the modification of the peripheral substituents in the *meso*-position of the porphyrin (the alkyne group of the free porphyrin was converted into the triazole moiety linked to the silica) as well as to the silica local environment [57]. As expected, the presence of only two Q-bands in the spectrum of metalated **EtTPPZn** (Figure S6, right) instead of the four bands characteristic of free-base porphyrins (Figure S6, left) clearly demonstrated that our procedure was efficient for totally removing zinc after the click reaction.

3.2 Characterization of hybrid materials

The obtained **N$_3$@SBA-15** and **TPPH$_2$@SBA-15** hybrid materials were fully characterised by bulk and molecular techniques to assess their textural, structural and integrity features.

The physicochemical and textural properties of hybrid materials resulting from powder XRD and sorption measurements are summarised in Table S1 (SI). Small angle powder XRD patterns of **N$_3$@SBA-15** before and after the click reaction with **EtTPPH$_2$** are displayed in Figure 1.

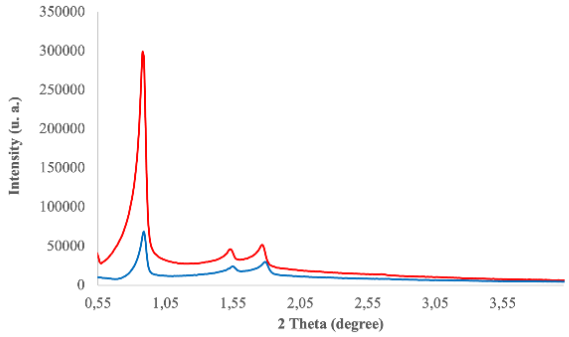

Fig. 1. X-ray powder diffraction patterns of azide functionalised silica material **N_3@SBA-15** and **$TPPH_2$@SBA-15**.

Both solids exhibited typical diffractograms in the 2θ-range of 0.5-3° characteristic of hexagonally mesophases. The presence of three well-resolved peaks that correspond to (100), (110) and (200) reflections as well as the absence of change of the unit-cell parameters a_0 (Table S1, SI) indicated that the post-functionalization click procedure did not diminish the structural long-range ordering of the solid. However, a significant decrease in intensity of the d_{100} reflection was observed after porphyrin incorporation, which could be attributed to lower local order and/or due to contrast matching between the amorphous silicate framework and the sterically encumbered porphyrin located inside the channels.

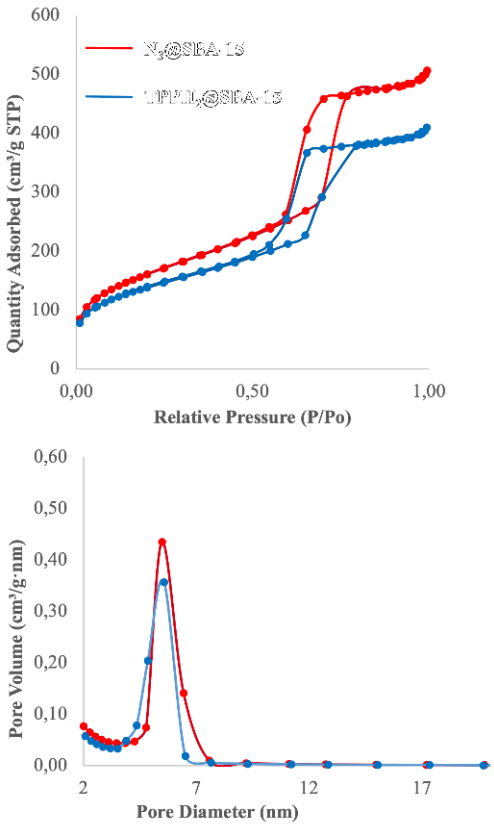

Fig. 2. Nitrogen adsorption/desorption isotherms (top) and pore size distributions (bottom) of **N_3@SBA-15** and **$TPPH_2$@SBA-15**.

Nitrogen adsorption-desorption measurements of **N_3@SBA-15** and **$TPPH_2$@SBA-15** hybrid materials showed a type IV isotherm typical of mesoporous solids. As visible in Figure 2, a well-defined sharp inflexion at a relative pressure range of 0.5 to 0.8 P/P_0 was shown for both solids although a marked decrease in N_2 uptake was observed for **$TPPH_2$@SBA-15**, which is consistent with the presence of bulky porphyrin in the pore channels and in agreement with the decrease of the SBET from 581 to 494 $m^2.g^{-1}$. Relatively narrow pore diameter distributions were obtained for both materials with a median pore diameter of 55 Å (Table S1, SI).

The successful ligation of the porphyrin moiety was confirmed by ^{13}C CP/MAS NMR spectroscopy. As shown in Figure 3, the peaks originating from the propyl chain of the azido tether can be clearly distinguished from those from the aromatic carbons of the porphyrin in the spectral region ranging respectively from 5 to 50 ppm and 110 to 160 ppm.

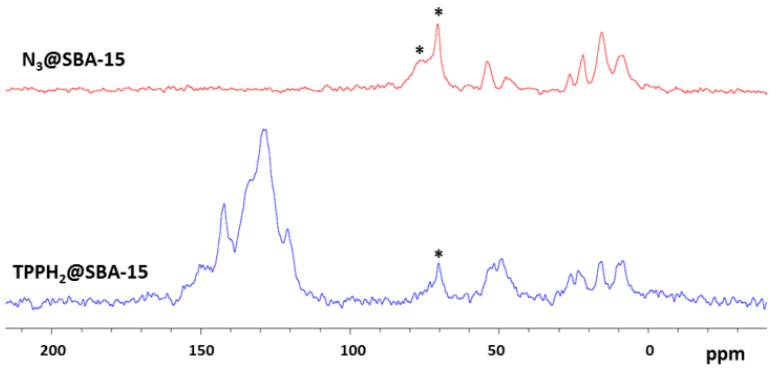

Fig. 3. ^{13}C CP/MAS NMR of **N_3@SBA-15** and **$TPPH_2$@SBA-15** hybrid materials. * Denotes for residual P123.

Solid-state ^{29}Si NMR provided further information regarding the silicon environment and the nature of the link to the surface. The presence of tertiary silicon peaks (55-75 ppm, $RSi\text{-}(OSi)_m\text{-}(OH)_{3-m}$, T-type sites) for both **N_3@SBA-15** and **$TPPH_2$@SBA-15** confirmed the presence of covalently bonded azidopropylsiloxane moieties (Figure S7, SI). The lack of significant changes in this spectral region was a clear indication that the covalent bonding of the tether in **N_3@SBA-15** was not affected upon the porphyrin attachment. Note that peaks assignable

to Q^2, Q^3 and Q^4 silicon sites of the silica frameworks (90-110 ppm) were also observed in both spectra.

A quantitative determination of organic content in the hybrid materials was deduced from nitrogen elemental analysis and, in order to ensure meaningful comparison, the organic loading was corrected from sample humidity by considering the SiO_2 content of the TGA run at 1000 °C (Figure S8 and Table S2, SI). Thus, the azidopropyl loading in **N_3@SBA-15** was found to be 0.24 mmol.g^{-1} dry silica and the porphyrin amount in **$TPPH_2$@SBA-15** was 0.11 mmol.g^{-1} dry silica, which corresponds to site density respectively of 0.24/nm^2 and 0.13/nm^2. This indicated that both functional groups are isolated as discrete molecular fragments onto the silica surface. The extent of click reaction was estimated to 46%, which was further confirmed by FT-IR by the marked decrease in intensity of the N_3 stretching vibration mode at 2111 cm^{-1} (Figure S9, SI).

3.3 Carbon dioxide cycloaddition to epoxides

In view of the efficiency of the **$TPPH_2$**/TBACl homogeneous binary system to promote the cycloaddition of carbon dioxide to aziridines forming oxazolidinones [50-51], a screening of the reaction parameters of the model reaction between styrene oxide (SO) and CO_2 was first undertaken under homogeneous conditions. This preliminary investigation was necessary for evaluating any beneficial effect due to the heterogenisation of the free-base porphyrin and for determining appropriate experimental conditions under which the heterogeneous catalytic system must be used.

Thus, to define the most convenient reaction time, the time dependent reaction profile of **$TPPH_2$**/TBACl binary system was evaluated under 1.2 MPa of CO_2, 125 °C and with a **$TPPH_2$**/TBACl/SO catalytic ratio of 1:5:10000. As shown in Figure S1 (SI), the yield of the cyclic product improved by increasing the reaction time up to 2.0 hours and then no further enhancement of the catalytic efficiency was observed.

The influence of the temperature on the catalytic performance (Figure S2, SI) was investigated by running the reaction for 1.5 h to better highlight the effect of the temperature on the reaction outcome prior reaching the plateau. Using the previously reported CO_2 pressure and catalytic ratio (1.2 MPa of CO_2 and **$TPPH_2$**/TBACl/SO = 1:5:10000), styrene carbonate **1** was only formed in traces when the reaction was run below 125 °C. The yield increased to 14% when the reaction was run at 150 °C and then, a decrease of the reaction productivity was observed at higher temperatures.

The molar ratio of the two components of the binary catalytic system, a key parameter impacting the overall reactivity, was in turn optimised. Figure S3 (SI) shows the dependence of the styrene carbonate yield on the **$TPPH_2$** concentration when the concentration of TBACl was maintained

constant at 0.05 mol%. Achieved results revealed a steadily increase of the styrene carbonate yield by increasing the **$TPPH_2$** concentration and the best result was obtained with a **$TPPH_2$**/TBACl molar ratio of 1:1. Finally, the dependence of the catalytic efficiency on the CO_2 pressure revealed that 0.6 MPa was sufficient to assure a good catalytic productivity (Figure S4, SI). As already reported [58], the decrease of the reaction yield observed at higher CO_2 pressures (0.9 and 1.2 MPa) could be due to the decrease of the epoxide concentration in the liquid phase, where the reaction takes place.

The optimised experimental conditions were then applied to investigate the catalytic influence of different ammonium salts (Table 1, entries 4-6). All the reactions were conducted for 1.0 hour in order to better appreciate the dependence of the catalytic activity on the nature of the used ammonium salt, since a longer duration could flatter catalytic effects.

As shown in Table 1, TBACl, used in combination with **$TPPH_2$**, was the most efficient among the tested ammonium salts and the comparison of runs 3 and 4 underlined the positive role of **$TPPH_2$**. In fact, both the reaction yield and TOF value almost doubled when **$TPPH_2$** was added to the catalytic mixture. It is important to note that the reaction did not proceed in the absence of any promoter (Table 1, entry 1) and the sole presence of the porphyrin was not sufficient to catalyse the reaction (Table 1, entry 2).

Table 1

Study of the effect of TBAX on the CO_2 cycloaddition to SO by using homogeneous **$TPPH_2$**/TBAX binary system.[a]

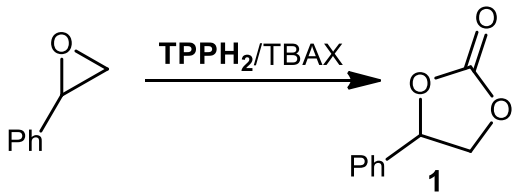

entry	porphyrin	TBAX	yield (%)[b]	TOF (h^{-1})[c]
1	/	/	0	/
2	**$TPPH_2$**	/	0	/
3	/	TBACl	11	228
4	**$TPPH_2$**	TBACl	20	416
5	**$TPPH_2$**	TBAB	14	291
6	**$TPPH_2$**	TBAI	9	187

[a)]Solvent-free reactions were run for 1.0 h by using 0.250 mL of SO at 150 °C, 0.6 MPa of CO_2 and **TPPH$_2$**/TBAX/SO = 5:5:10000; [b)]yields were measured by ^{1}H NMR spectroscopy by using 2,4-dibromomesitylene as the internal standard. All the reactions occurred with 100% of selectivity; [c)]turnover frequencies (TOF) are related to either porphyrin or ammonium salt, as their concentrations are equivalent.

Then, the reaction scope was investigated by testing different epoxides under the optimised experimental conditions. Results, which were achieved by running solvent-free reactions for 2.0 h at 150 °C, 0.6 MPa of CO_2 and **TPPH$_2$**/TBACl/epoxide ratio of 5:5:10000, are listed in the first three columns of Table 2. All the reactions, except the synthesis of compounds **6** and **7**, were performed by using both 0.250 mL and 5.0 mL of substrate to verify if it was possible scaling up the procedure for further process developments. Even if the turnover number (TON) and turnover frequency (TOF) values were very high for a metal-free catalytic system, all the compounds were obtained in moderate to low yields. While the best yield of 64% was registered for the synthesis of **3**, compounds **1** and **2** were obtained in similar moderate yields.

Table 2

Scope of the CO_2 cycloaddition to epoxides under homogeneous **TPPH$_2$**/TBACl (**A**) and heterogeneous **TPPH$_2$@SBA-15**/TBAI (**B**) conditions.[a]

	Homogeneous conditions (**A**)[b] **TPPH$_2$**/TBACl			Heterogeneous conditions (**B**)[c] **TPPH$_2$@SBA-15** /TBAI		
product	**yield %[d]**	**TON**	**TOF (h^{-1})**	**yield %[d]**	**TON**	**TOF (h^{-1})**
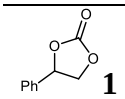 **1**	36 (34[e])	720 (707[e])	360 (354[e])	42	832	416
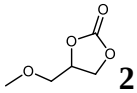 **2**	39 (34[e])	774 (728[e])	387 (364[e])	41	814	407
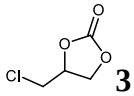 **3**	64 (50[e])	1280 (998[e])	640 (499[e])	80	1600	800
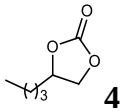 **4**	16 (15[e])	331 (312[e])	166 (156[e])	30	621	311
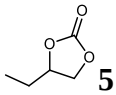 **5**	12 (14[e])	287 (334[e])	144 (168[e])	26	533	266

 **6**	5	40	20	traces	traces	traces
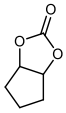 **7**	4	82	41	traces	traces	traces
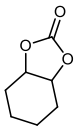 **8**	5 (4[e])	102 (83[e])	51 (42[e])	traces	traces	traces

[a)]Solvent-free reactions were run for 2.0 h by using 0.250 mL of epoxide at 150 °C, 0.6 MPa of CO_2; [b)]**TPPH$_2$**/TBACl/epoxide = 5:5:10000. [c)]**TPPH$_2$@SBA-15**/TBAI/epoxide = 5:5:10000; [d)]yields were measured by ^{1}H NMR using 2,4-dibromomesitylene as the internal standard. All the reactions occurred with 100% of selectivity; [e)]5.0 mL of epoxide were used.

Unfortunately, all the other compounds were obtained in very low yields and reported data did not underline a dependence of the reaction performance on the length of the alkyl chain present on the epoxide ring (compare yields of compounds **4** and **5**). Epoxides presenting a quaternary carbon atom as well as bicyclic epoxides were almost unreactive and compounds **6**, **7** and **8** were formed in very low yields. As shown in Table 2, the reaction productivity did not change by scaling up the reaction and similar yields were observed by using either 0.250 or 5.0 mL (yield value in brackets) of epoxide.

Having in mind data reported above, the activity of the porphyrin-functionalised silica **TPPH$_2$@SBA-15** was tested in the model reaction of SO with CO_2. TBACl was first chosen as ammonium salt counterpart due to its reactivity under optimised homogeneous conditions.

The yield in styrene carbonate drastically decreased from 20 to 6% when the homogeneous system was replaced by the heterogeneous one (compare entry 4 of Table 1 with entry 1 of Table 3) As already reported [59], this negative effect could arise from the formation of hydrogen bonding between the silanols of the silica surface and the basic chloride anion, which reduced its nucleophilicity and in turn the catalytic efficiency of the whole system.

Table 3

Study of the reaction between SO and CO_2 under heterogeneous conditions.[a]

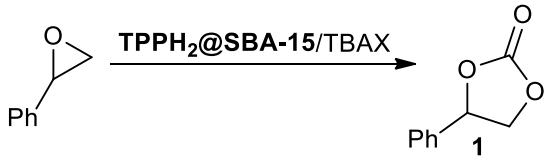

entry	X	Lewis Acid	yield (%)[b]	TOF (h^{-1})
1	Cl	**$TPPH_2$@SBA-15**	6	59
2	I	**$TPPH_2$@SBA-15**	42 (28[c])	416 (555[c])
3	I	**EtTPPZn@SBA-15**	33	331
4	I	**N_3@SBA-15**	34 (15[c])	337 (297[c])
5	I	**N_3@SBA-15** + **$TPPH_2$**	23	228
6	I	**SBA-15**	31	313
7	I	**Regular silica**	29	292
8	I	/	15 (5[c])	148 (99[c])

[a)]Solvent-free reactions were run for 2.0 h by using 0.250 mL of epoxide at 150 °C, 0.6 MPa of CO_2 and LA/TBAX/SO = 5:5:10000; [b)]measured by ^{1}H NMR using 2,4-dibromomesitylene as the internal standard. All the reactions occurred with 100% of selectivity; [c)]after 1.0 h of reaction.

The replacement of TBACl with TBAI (entry 2, Table 3) had a marked positive effect due to the presence of the less basic iodide anion that, being less prone to form hydrogen bonds with the solid support, maintained the required nucleophilicity for the ring opening reaction. Yields, TON and TOF values increased by a factor of seven when TBACl was substituted by TBAI highlighting the crucial role of the interactions between silanols of the slightly acidic surface and halide anions. When the synthesis of styrene carbonate was performed by replacing the **$TPPH_2$@SBA-15**/TBAI system (entry 2, Table 3) with a combination of TBAI with **EtTPPZn@SBA-15** (entry 3, Table 3) or the sole azido-functionalised silica **N_3@SBA-15** (entry 4, Table 3) or **N_3@SBA-15**/$TPPH_2$ mixture (entry 5, Table 3), lower yields were obtained (33%, 34% and 23%, respectively). Analogously, product **1** was formed in the lower yield of 31% and 29% when TBAI was used in the presence of either unfunctionalised **SBA-15** (entry 6, Table 3) or the regular column chromatography silica (entry 7, Table 3), respectively.

It should be stressed that the intrinsic catalytic capacity of the sole TBAI was enhanced by the presence of porphyrin to confirm the catalytic role of the porphyrin heterogenised onto the silica support in promoting the CO_2 cycloaddition to SO (compare entries 2 and 8, Table 3). On the other hand, the cycloaddition did not proceed with the exclusive presence of either **$TPPH_2$@SBA-15** or **EtTPPZn@SBA-15** material as well as in the presence of functionalised **N_3@SBA-15** or unmodified **SBA-15** and regular silica, highlighting the crucial role of the ammonium salt for the reaction outcome.

Once the activity of the catalytic **TPPH$_2$@SBA-15**/TBAI system was confirmed, the reaction scope was investigated by testing the same substrates which were used under homogeneous conditions and obtained results are listed in columns 4, 5 and 6 of Table 2.

Even if the general trend discussed above was confirmed when using the silica-based material, diffusion constraints played an important role under heterogeneous conditions, as revealed by the lack of the formation of products **6**, **7**, and **8**. The high steric hindrance of corresponding epoxides was probably not compatible with the free space around the active site in the heterogeneous material and hampered the reaction to progress.

On the other hand, it was very interesting noting that the synthesis of compounds **1-5** was more productive by using **TPPH$_2$@SBA-15** instead of **TPPH$_2$** as the promoter. Yields, TON and TOF values were higher than those obtained under homogenous conditions (compare data in Table 2) suggesting the key role of silanols in activating epoxide *via* hydrogen bonding. Note that registered TON and TOF values were remarkable for a metal-free heterogeneous catalytic CO_2 cycloaddition.

Considering that one of the most important advantages of using a heterogeneous catalyst is the possibility to easily recover it, the recyclability of the **TPPH$_2$@SBA-15** system was investigated by performing three consecutive gram-scale cycloadditions of carbon dioxide to 1.0 gram of SO. The heterogeneous material was recovered after each run by a simple filtration and the desired product **1** was obtained in 30%, 34% and 31% yield, respectively. Even if a slight decrease of the yields was detected in all the three performed reactions, these results testified the chemical stability and the recyclability of the hybrid material. It should be noted that when the carbon dioxide cycloaddition to 1.0 gram of SO was performed in the presence of the **N$_3$@SBA-15**/TBAI system, compound **1** was obtained in the lower yield of 16% confirming the beneficial role of porphyrin in the reaction

The low porphyrin leaching of 0.7% was detected by UV-Vis spectroscopy to indicate the good chemical stability of the porphyrin-support linkage. Considering that at this low concentration the porphyrin activity is negligible, it is possible to state that the synthesis of epoxides was only mediated by the heterogenised porphyrin.

Thus, the use of **TPPH$_2$@SBA-15**/TBAI catalytic system allowed enhancing catalytic performances with respect to homogeneous catalytic systems thanks to the synergic role of the solid support in activating epoxides. The good recyclability and the possibility to scaling up the reaction paved the way to further process developments such as performing reactions under continuous-flow conditions, which can be of particular importance for a solvent-free procedure occurring with a 100% atom economy. Desired products can be continuously formed and the

drawback of producing low yields of cyclic carbonates by a single synthetic loop could be circumvented.

3.4. Carbon dioxide cycloaddition to aziridines

In view of the results obtained reacting epoxides and CO_2 in the presence of the heterogeneous **TPPH$_2$@SBA-15**/TBAI catalytic system, this hybrid material was also tested in the cycloaddition of carbon dioxide to aziridines forming *N*-alkyl oxazolidinones. First, the reactivity of *N*-alkyl derivatives was analysed by testing 1-butyl-2-phenyl aziridine **9** as a model substrate and results are listed in Table 4. Since aziridines are generally less reactive than epoxides [60], we increased the amount of **TPPH$_2$@SBA-15** to 0.4 mol% and 2.0 mol% for TBAI. It should be noted that, contrarily to what occurs in the CO_2 cycloaddition to epoxides, the reaction of aziridines leads to the formation of two different regioisomers **a** and **b**, depending on which aziridine carbon atom is attacked by the nucleophilic species (Scheme 3).

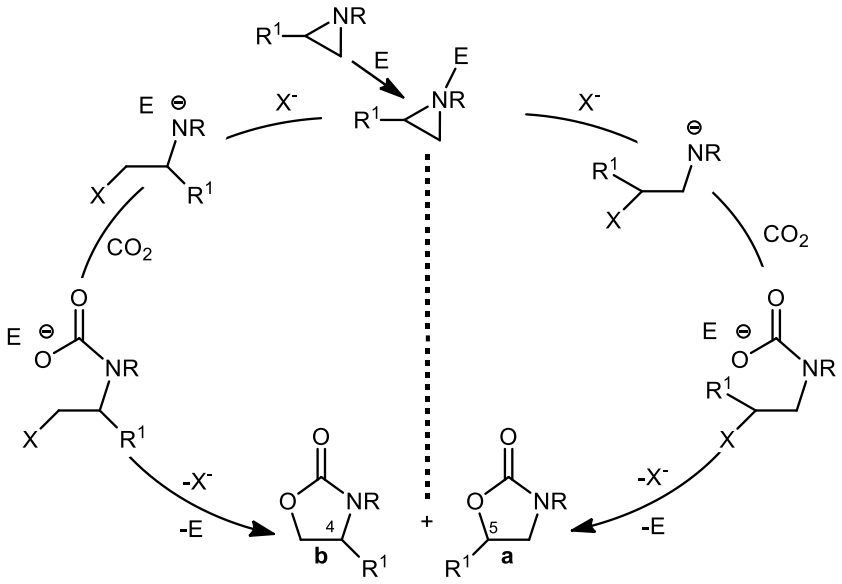

Scheme 3. General scheme of the CO_2 cycloaddition to aziridines promoted by E/TBAX system (E = electrophile) forming the two oxazolidinone regioisomers **a** and **b**.

It should be noted that while TBAI alone can activate **9** towards the formation of **10a**/**10b** mixture in a low yield and acceptable regioselectivity (entry 1, Table 4), the reaction did not proceed in the presence of the sole **TPPH$_2$** or the hybrid **TPPH$_2$@SBA-15** material or the binary **N$_3$@SBA-15**/**TPPH$_2$** system. These results underlined once again the catalytic importance of the ammonium salt in the CO_2 cycloadditions.

Table 4.

Optimization of the carbon dioxide cycloaddition to aziridine **9**.[a]

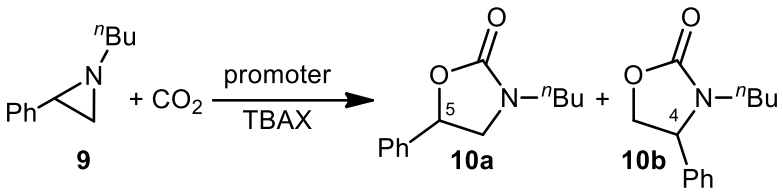

9 **10a** **10b**

entry	promoter	TBAX	t (h)	yield (%)[b]	a/b ratio[b]
1	/	TBAI	1	9	87/13
2	**N_3@SBA-15**	TBAI	1	17	90/10
3	**$TPPH_2$@SBA-15**	TBAI	1	25	99/1
4	**$TPPH_2$**	TBAI	1	42	98/2
5	/	TBACl	1	65	86/14
6	**$TPPH_2$@SBA-15**	TBACl	1	20	98/2
7	/	TBAI	6	75	92/8
8	**$TPPH_2$@SBA-15**	TBAI	6	95	97/3
9	**$TPPH_2$@SBA-15**	TBACl	6	81	95/5

[a]1.5 M aziridine THF solution in a steel autoclave at 125 °C, 1.2 MPa of CO_2 and promoter/TBAX/aziridine = 1:5:250; [b]calculated by ^{1}H NMR spectroscopy by using 2,4-dinitrotoluene as the internal standard. All the reactions occurred with 100% of selectivity.

When TBAI was utilised in combination with **N_3@SBA-15**, an improvement of the product yield was obtained with respect to the yield of the reaction performed by using TBAI alone (compare entries 1 and 2 of Table 4) suggesting that silica operated synergistically with the ammonium salt also in the case of the aziridine activation. A further increase of the reaction yield and regioselectivity was registered in the presence of **$TPPH_2$@SBA-15**/TBAI thanks to the positive catalytic effect of the porphyrin in the reaction outcome (entry 3, Table 4).

Contrarily to what was observed in the cycloaddition to epoxides, the heterogeneous catalytic system was less active than the homogeneous binary system (compare entries 3 and 4 of Table 4). This could be due to limited aziridine activation through hydrogen bonding between nitrogen atom and silanols of the support owing to the high steric hindrance around the nitrogen aziridine atom.

Then, TBACl was tested as LB both alone and in combination with **$TPPH_2$@SBA-15** (entries 5 and 6, Table 4). Acquired data indicated that the reactivity of TBACl was reduced in presence of silica, since the reaction yield dropped from 65% to 20%. However, the presence of porphyrin had a positive effect on the reaction regioselectivity. As already reported for the cycloaddition to

epoxides, TBAI was the most efficient TBAX, as revealed by reactions run for 6 hours in the presence of either **TPPH$_2$@SBA-15**/TBAI or **TPPH$_2$@SBA-15**/TBACl catalytic systems (compare entries 8 and 9 of Table 4).

The catalytic combination **TPPH$_2$@SBA-15**/TBAI was selected as the most efficient for studying the scope of the conversion of *N*-alkyl aziridines into corresponding *N*-alkyl oxazolidinones.

Some reactions were performed for either 6 or 16 h to better compare the reactivity of the starting aziridines. Achieved data are summarised in Table 5.

Table 5

Scope of the CO_2 cycloaddition to *N*-alkyl aziridines.[a]

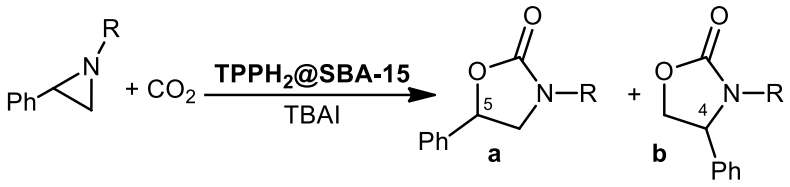

entry	R	yield (%)[b]	**a/b** ratio[b]
1	^{n}butyl	100 (95)[c]	**10a**/**10b** = 94/6 (97/3)[c]
2	^{i}butyl	86 (28)[c]	**11a**/**11b** = 99/1 (99/1)[c]
3	^{s}butyl	34 (5)[c]	**12a**/**12b** = 99/1 (99/1)[c]
4	^{t}butyl	/	/
5	cyclopentyl	97 (34)[c]	**13a**/**13b** = 99/1 (99/1)[c]
6	cyclohexyl	42 (8)[c]	**14a**/**14b** = 99/1 (99/1)[c]
7	methylcyclohexyl	95 (30)[c]	**15a**/**15b** = 99/1 (99/1)[c]
8	benzyl	100 (42)[c]	**16a**/**16b** = 99/1 (99/1)[c]
9	4-methoxy benzyl	100 (48)[c]	**17a**/**17b** = 99/1 (99/1)[c]
10	^{i}amyl	100 (67)[c]	**18a**/**18b** = 93/7 (94/6)[c]
11[d]	^{n}butyl	88	**10a**/**10b** = 93/7
12[e]	^{n}butyl	100	**10a**/**10b** = 93/7
13[f]	^{n}butyl	100	**10a**/**10b** = 94/6
14[g]	^{n}butyl	100	**10a**/**10b** = 94/6
15[h]	^{n}butyl	100	**10a**/**10b =** 93/7

[a)]1.5 M aziridine THF solution in a steel autoclave with **TPPH$_2$@SBA-15**/TBAI/aziridine = 1:5:250 at 125 °C and 1.2 MPa of CO_2 for 16 h; [b)]obtained by ^{1}H NMR using 2,4-dinitrotoluene as the internal standard. All the reactions occurred with 100% of selectivity; [c)]reactions run for 6 h; [d)]solvent-free reactions with **TPPH$_2$@SBA-15**/TBAI/aziridine = 1:5:400; [e)]first recycle; [f)]second recycle; [g)]third recycle; [h)]reaction performed with 1.0 g of substrate.

Considering that the steric encumbrance on the nitrogen atom is the most important factor which influenced the reaction productivity, different aziridines presenting different alkyl chains on the nitrogen atom were tested (entries 1-4, Table 5). Experimental results showed that the reaction yield proportionally decreased by augmenting the bulkiness of the R substituent bonded to the aziridine nitrogen atom (entries 1-3, Table 5), as clearly indicated by the complete lack of reactivity of *1-tert*-butyl-2-phenyl aziridine (entry 4, Table 5). The negative effect was less evident when a CH_2 spacer was present between the sterically hindered group and the nitrogen atom, as supported by data acquired in the synthesis of compounds **15-18** (entries 7-9 of Table 5). However, all these substrates were less reactive than aziridine **9** when the reaction was run for the reduced time of 6 hours. The comparison between entries 2 and 10 (Table 5) suggested that the relocation of the steric encumbrance on one carbon atom forward may be sufficient to drastically improve the reaction productivity (from 28 to 67% yield after 6 hours of reaction).

The reaction was also efficient with aziridine bearing cyclic alkyl group on the nitrogen atom. *N*-cyclopentyl substituted product **13** was obtained in a yield higher than that achieved in the synthesis of **14** probably due to the flatter character of the cyclopentyl substituent with respect to the cyclohexyl one, which reduced the steric hindrance around the nitrogen atom. It is important to underline that all the reactions displayed a very good regioisomeric ratio, up to 99/1 and never lower than 94/6.

The synthesis of **10** was also tested under solvent-free conditions and, despite the slight reduction of the yield (from 100% in entry 1 to 88% yield in entry 11, Table 5), this result can be considered as a starting point for further decreasing the environmental impact of the protocol by avoiding the use of organic solvents.

The material recyclability was also investigated by performing four consecutive experiments with the same **TPPH$_2$@SBA-15** material that, after every reaction, was simply filtered, washed with dichloromethane, dried in the oven and re-used (entries 12-14, Table 5). All the reactions occurred with a complete substrate conversion, full selectivity and the same regioselectivity showed by the fresh material. Finally, the carbon dioxide cycloaddition to **9** was performed in a larger scale by using 1.0 gram of substrate and, to our delight, the reaction occurred with 100% of yield. The recyclability of the material and its efficiency when working on a large scale could open the doors to the practical applications of the procedure.

Motivated by the good results obtained reacting epoxides and *N*-alkyl aziridines with carbon dioxide, we also tested the heterogeneous system **TPPH$_2$@SBA-15**/TBAI with the more challenging *N*-aryl aziridines. The cycloaddition of CO_2 to

1-(3,5-*bis*(trifluoromethyl)phenyl)-2-phenyl aziridine **19**, utilising the **TPPH$_2$@SBA-15**/TBAI/substrate ratio of 1:5:100 under the experimental conditions reported above, proceeded with a very low selectivity towards the formation of the desired oxazolidinone despite the complete conversion of the starting aziridine. Fortunately, the simple replacement of TBAI with TBACl resulted in an enhancement of the catalytic efficiency and a complete conversion of **19** into the desired oxazolidinone **20**.

Thus, to better investigate the effect of TBAX in the synthesis of oxazolidinones catalysed by **TPPH$_2$@SBA-15**/TBAX system, the *N*-alkyl aziridine **9** and the *N*-aryl aziridine **19** were reacted with carbon dioxide in the presence of both TBACl and TBAI (Figure 4).

As reported in Figure 4a, even if the reaction of **9** with carbon dioxide produced **10** in the same extent after 16 hours in the presence of both the ammonium salts, TBAI resulted more efficient in terms of the reaction rate. A reverse result was observed in the CO_2 cycloaddition to *N*-aryl aziridines where a marked decrease of the reaction productivity was observed when TBAI was employed.

Considering the double role of halide anion in the reaction, being both the nucleophilic species responsible for the ring-opening reaction of the aziridine and the leaving-group that allows the ring-closing step occurring (Scheme 3), a balance of these two abilities determines the overall activity of the ammonium salt.

Thus, the activity of TBAX can depend on electronic and steric characteristics of the aziridine substrate as well as the reaction conditions [61]. It is necessary to better study the mechanism of this reaction to understand the difference in reactivity that was observed by using either TBAI or TBACl in the CO_2 cycloaddition to *N*-aryl aziridines. We suggest that the higher steric hindrance of *N*-aryl with respect to *N*-alkyl aziridine, around the nitrogen atom, can be responsible for a worse approach of the anion during the ring-opening step. This negative effect can be more pronounced for I^- rather that Cl^- and it could explain why TBACl is a better nucleophilic source than TBAI in the case of the CO_2 cycloaddition to *N*-aryl aziridines.

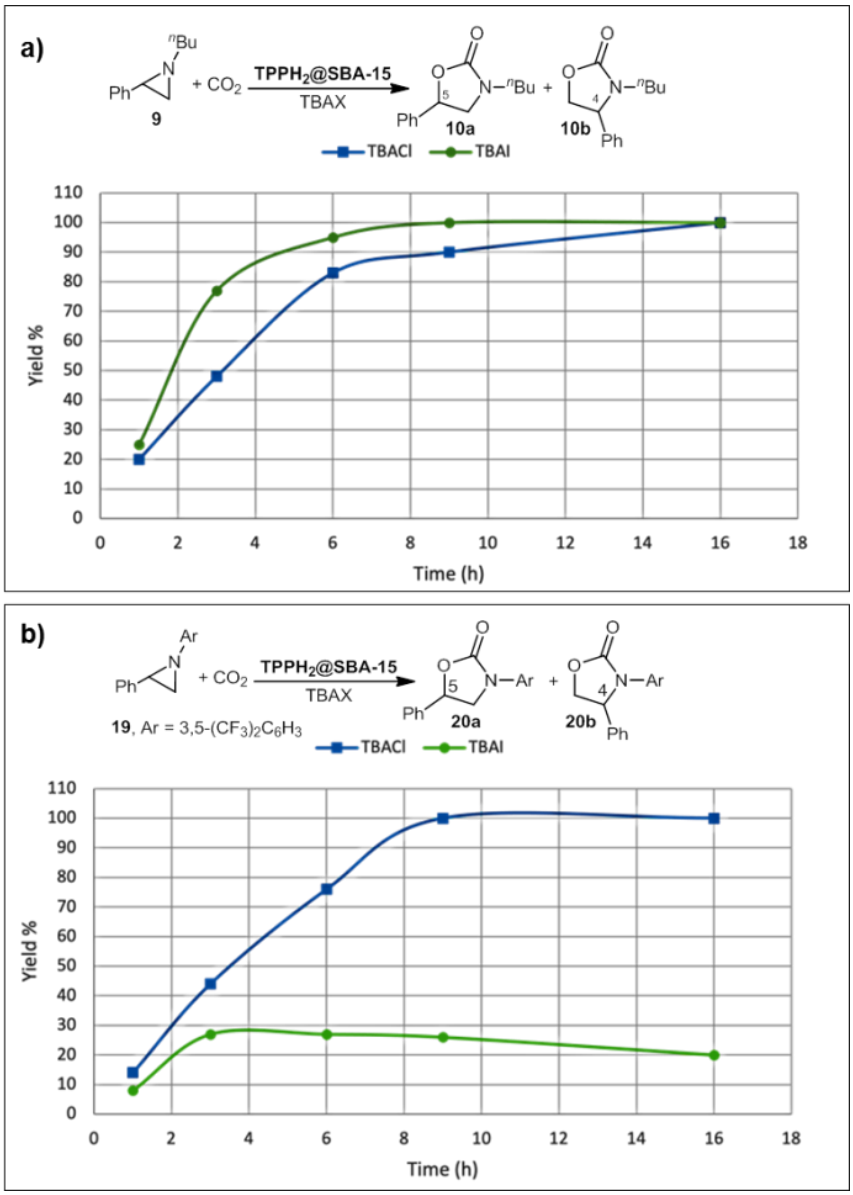

Fig. 4. TBAX activity in the cycloaddition reaction of CO_2 to **9** (Fig. 4a) and **19** (Fig. 4b). All the reactions were performed with 1.5 M aziridine THF solution in a steel autoclave with **TPPH$_2$@SBA-15**/TBAX/aziridine ratio of 1:5:250 (Fig. 4a) and 1:5:100 (Fig. 4b) at 125 °C and 1.2 MPa of CO_2. Yields calculated by ^{1}H NMR with 2,4-dinitrotoluene as the internal standard.

In view of what discussed above, the scope of the synthesis of *N*-aryl oxazolidinones was investigated by using **TPPH$_2$@SBA-15**/TBACl binary system even if the halide efficiency can be reduced by the interaction with the silica matrix. Thus, several reactions were performed at 125 °C and 1.2 MPa for 16 h by using the **TPPH$_2$@SBA-15**/TBACl/aziridine ratio of 1:5:100.

As reported in Table 6, the employed catalytic system performed well by employing aziridines presenting electron-poor Ar groups on the aziridine nitrogen atom (entries 1-4 and 8, Table 6), independently from the electronic nature of Ar'. Even if the reaction producing **23a**/**23b** mixture was quantitative, the regioselectivity was quite low (entry 4, Table 6). The presence of either a

halogen or an EDG group on the Ar substituent was responsible for a decrease of the reaction yield with no effect on the reaction regioselectivity (entries 6, 7 and 9, Table 6).

The moderate yield, associated with a moderate regioselectivity, for the synthesis of **24** can be mainly due to negative steric effects rather that the presence of an electron-deficient Ar' group.

The recyclability and chemical robustness of the immobilised porphyrin was tested by repeating the synthesis of compound **20** four consecutive times by using the same heterogeneous material which was filtered, washed and dried before each new catalytic cycle. The desired compound was obtained in very good yields and regioselectivities, as reported in entries 10-12 of Table 6 and no remarkable differences were observed with respect to the reaction performed with the fresh material (entry 1, Table 6). Achieved data indicated that the reported hybrid material was reusable up to four times without any lack of reactivity.

Finally, the same reaction was performed on a larger scale by using 1.0 g of substrate and the desired product was formed in quantitative yield. Only a minor lowering of the regioselectivity was detected (entry 13, Table 6). The data suggested the possibility to apply this heterogeneous catalytic system to further process development.

In conclusion, the porphyrin-functionalised silica displayed very good activity for the conversion of several substituted *N*-aryl aziridines, even in large scale, and the good selectivity towards the synthesis of 5-substituted *N*-aryl oxazolidinone **a** was coupled to the facility in reusing **TPPH$_2$@SBA-15** to enhance the process sustainability.

Table 6

Reaction scope of the carbon dioxide cycloaddition to *N*-aryl aziridines.[a]

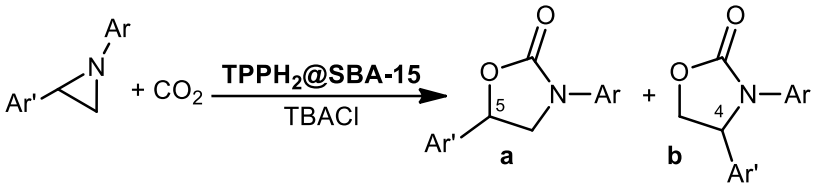

entry	Ar	Ar'	Conversion (%)[b]	Selectivity (%)[b]	Yield (%)[b]	a/b ratio[b]
1	3,5-$(CF_3)_2C_6H_3$	C_6H_5	100	100	100	**20a**/**20b** = 93:7
2	3,5-$(CF_3)_2C_6H_3$	4-^{t}BuC_6H_4	97	100	97	**21a**/**21b** = 93:7
3	3,5-$(CF_3)_2C_6H_3$	4-MeC_6H_4	96	99	95	**22a**/**22b** = 99:1
4	3,5-$(CF_3)_2C_6H_3$	4-BrC_6H_4	100	100	100	**23a**/**23b** = 75:25
5	3,5-$(CF_3)_2C_6H_3$	C_6F_5	55	100	55	**24a**/**24b** = 83:17
6	4-BrC_6H_4	C_6H_5	64	98	63	**25a**/**25b** = 99:1
7	4-ClC_6H_4	C_6H_5	66	100	66	**26a**/**26b** = 98:2
8	4-NO_2 C_6H_4	C_6H_5	100	100	100	**27a**/**27b** = 85:15
9	4-^{t}Bu C_6H_4	C_6H_5	100	20	20	**28a**/**28b** = 99:1
10[c]	3,5-$(CF_3)_2C_6H_3$	C_6H_5	100	100	100	**20a**/**20b** = 92:8
11[d]	3,5-$(CF_3)_2C_6H_3$	C_6H_5	96	100	96	**20a**/**20b** = 96:4
12[e]	3,5-$(CF_3)_2C_6H_3$	C_6H_5	100	100	100	**20a**/**20b** = 93:7
13[f]	3,5-$(CF_3)_2C_6H_3$	C_6H_5	100	100	100	**20a**/**20b** = 86:14

[a)]1.5 M aziridine THF solution in a steel autoclave with **TPPH$_2$@SBA-15**/TBACl/aziridine = 1:5:100 at 125 °C and 1.2 MPa of CO_2 for 16 h; [b)]obtained by ^{1}H NMR by using 2,4-dinitrotoluene as the internal standard; [c)]first recycle; [d)]second recycle; [e)]third recycle; [f)]reaction performed with 1.0 gram of substrate.

4. Conclusion

A heterogeneous material for the carbon dioxide cycloaddition to three membered heterocycles was prepared by immobilising a free-base porphyrin onto high surface area SBA-15 silica through robust covalent triazole linkages. The characterization of resulting **TPPH$_2$@SBA-15** indicated the structural integrity of the mesoporous host after anchoring the porphyrin molecule as a discrete species. The so-obtained material was applied to promote the reaction of epoxides, *N*-alkyl and *N*-aryl aziridines towards carbon dioxide in the presence of quaternary ammonium halides.

The conversion of epoxides into cyclic carbonates performed better in the presence of the heterogeneous **TPPH$_2$@SBA-15**/TBAI catalytic system with respect to catalytic reactions

promoted by the all soluble **TPPH$_2$**/TBACl combination. The heterogeneous material worked well at low loading (0.05 mol%) and short reaction time (2 hours) with TOF values ranging from 266 to 800 h^{-1}.

Then, **TPPH$_2$@SBA-15**/TBAI catalytic system was applied to mediate the more challenging conversion of *N*-alkyl aziridines into *N*-alkyl oxazolidinones. Different *N*-alkyl aziridines were successfully reacted with carbon dioxide stating the dependence of the reaction productivity on steric factors.

Finally, by replacing TBAI with TBACl, the heterogeneous system performed well in converting the less reactive *N*-aryl aziridines into the corresponding *N*-aryl oxazolidinones. It should be noted that this is the first example of a heterogeneous version of this organic transformation and excellent yields and remarkable regioselectivities were obtained.

The recyclability of **TPPH$_2$@SBA-15** was assessed in all the studied organic transformations to support the excellent chemical stability of the heterogeneous material that did not lose its activity due to leaching processes or decomposition pathways. These results, together with the possibility to conduct the reaction in a gram-scale by maintaining the same catalytic efficiency, render this methodology a promising route to further process developments.

In order to further enhance the sustainability and productivity of this metal-free heterogeneous process, we are currently investigating the continuous-flow chemical ("flow chemistry") reaction of CO_2 with epoxides and aziridines. The injection of reactants through reactors in a continuous fashion can be of a particular importance for a solvent-free procedure that occurs with 100% of the atom economy.

Acknowledgements

PS gratefully acknowledges the Erasmus+ project for the traineeship granted that made possible the collaboration between University of Milan and University of Lyon.

Supplementary material

SI contains general conditions, preparation of reagents, experimental details for the synthesis and characterisation of heterogeneous material as well as all organic products and copies of NMR spectra.

References

[1] N. Jones, Nat. Geosci., 6 (2013) 589-589.

[2] M. Bui, C. S. Adjiman, A. Bardow, E. J. Anthony, A. Boston, S. Brown, P. S. Fennell, S. Fuss, A. Galindo, L. A. Hackett, J. P. Hallett, H. J. Herzog, G. Jackson, J. Kemper, S. Krevor, G.

C. Maitland, M. Matuszewski, I. S. Metcalfe, C. Petit, G. Puxty, J. Reimer, D. M. Reiner, E. S. Rubin, S. A. Scott, N. Shah, B. Smit, J. P. M. Trusler, P. Webley, J. Wilcox, N. Mac Dowell, Energ. Environ. Sci., 11 (2018) 1062-1176.

[3] O. Akeeb, L. Wang, W. Xie, R. Davis, M. Alkasrawi, S. Toan, J. Environ. Manage., 313 (2022) 115026.

[4] C. B. Agaton, Sci. Total Environ., 795 (2021) 148683.

[5] J. A. Martens, A. Bogaerts, N. De Kimpe, P. A. Jacobs, G. B. Marin, K. Rabaey, M. Saeys, S. Verhelst, ChemSusChem, 10 (2017) 1039-1055.

[6] Q. W. Song, Z. H. Zhou, L. N. He, Green Chem., 19 (2017) 3707-3728.

[7] A. I. Osman, M. Hefny, M. I. A. Abdel Maksoud, A. M. Elgarahy, D. W. Rooney, Environ. Chem. Lett., 19 (2021) 797-849.

[8] Q. Liu, L. Wu, R. Jackstell, M. Beller, Nat. Commun., 6 (2015) 5933.

[9] C. C. Truong, D. K. Mishra, Environ. Chem. Lett., 19 (2021) 911-940.

[10] A. W. Kleij, M. North, A. Urakawa, ChemSusChem, 10 (2017) 1036-1038.

[11] R. R. Shaikh, S. Pornpraprom, V. D'Elia, ACS Catal., 8 (2018) 419-450.

[12] A. Rehman, F. Saleem, F. Javed, A. Ikhlaq, S. W. Ahmad, A. Harvey, J. Environ. Chem. Eng., 9 (2021), 105113.

[13] E. J. C. Lopes, A. P. C. Ribeiro, L. M. D. R. S. Martins, Catalysts, 10 (2020) 479.

[14] S. Arshadi, A. Banaei, S. Ebrahimiasl, A. Monfared, E. Vessally, RSC Advances, 9 (2019) 19465-19482.

[15] J. K. Lamb, D. V. I. Ingram, M. North, M. Sengoden, Curr. Green Chem., 6 (2019) 32-43.

[16] S. Pulla, C. M. Felton, P. Ramidi, Y. Gartia, N. Ali, U. B. Nasini, A. Ghosh, J. CO2 Util., 2 (2013) 49-57.

[17] C. C. Truong, D. K. Mishra, Environ. Chem. Lett., 19 (2021) 911–940

[18] L. Xiao-Fang, W. Mei-Yan, H. Liang-Nian, Curr. Org. Chem. 21 (2017) 698-707.

[19] T. D. Hu, Y. H. Ding, Organometallics, 39 (2020) 505-515.

[20] W. McGhee, D. Riley, K. Christ, Y. Pan, B. Parnas, J. Org. Chem., 60 (1995) 2820-2830.

[21] A. A. G. Shaikh, S. Sivaram, Chem. Rev., 96 (1996) 951-976.

[22] B. Schäffner, F. Schäffner, S. P. Verevkin, A. Börner, Chem. Rev., 110 (2010) 4554-4581.

[23] C. Claver, M. B. Yeamin, M. Reguero, A. M. Masdeu-Bultó, Green Chem., 22 (2020) 7665-7706.

[24] D. A. Evans, J. Bartroli, T. L. Shih, J. Am. Chem. Soc., 103 (1981) 2127-2129.

[25] Z. Vahideh, M. H. Majid, Curr. Org. Synth., 15 (2018) 3-20.

[26] C. Roger, J. A. Roberts, L. Muller, Clin. Pharmacokinet., 57 (2018) 559-575.

[27] T. Niemi, T. Repo, Eur. J. Org. Chem. (2019) 1180-1188.

[28] X. Wu, J. A. Castro-Osma, M. North, Symmetry, 8 (2016) 4.

[29] R. L. Paddock, S. T. Nguyen, J. Am. Chem. Soc., 123 (2001) 11498-11499.

[30] X.-D. Lang, L.-N. He, Chem. Rec., 16 (2016) 1337-1352.

[31] M. Cavalleri, N. Panza, A. di Biase, G. Tseberlidis, S. Rizzato, G. Abbiati, A. Caselli, Eur. J. Org. Chem. (2021) 2764-2771.

[32] M. Alonso de la Peña, L. Merzoud, W. Lamine, A. Tuel, H. Chermette, L. Christ, J. CO2 Util., 44 (2021) 101380.

[33] a) D. Intrieri, C. Damiano, P. Sonzini, E. Gallo, J. Porphyrins Phthalocyanines, 23 (2019) 305-328. b) J. Yi, S. Sun, Z. Li, X. Gao, X. Sun, N. Wang, J. Li, Appl. Organomet. Chem., 34 (2020) e5382

[34] a) N. Sharma, S. S. Dhankhar, C. M. Nagarajia, Microporous Mesoporous Mater., 280 (2019) 372-378. b) J. Liang, Y-.Q. Xie, Q. Wu, X.-Y. Wang, T.-T. Liu, H.-F. Li, Y.-B. Huang, R. Cao, Inorg. Chem. 57 (2018) 2584-2593. c) M. H. Kim, T. Song, U. R. Seo, J. E. Park, K. Cho, S. M. Lee, H. J. Kim, Y.-J. Ko, Y. K. Chung, S. U. Son, J. Mater. Chem. A, 5 (2017) 23612-23619. d) T. Ema, Y. Miyazaki, T. Taniguchi, J. Takada, *Green Chem.* 15 (2013) 2485-2492.

[35] a) M. Cokoja, M. E. Wilhelm, M. H. Anthofer, W. A. Herrmann, F. E. Kühn, ChemSusChem, 8 (2015) 2436-2454. b) X. Wu, C. Chen, Z. Guo, M. North, A. C. Withwood, ACS Catal. 9 (2019) 1895-1906.

[36] V. Caló, A. Nacci, A. Monopoli, A. Fanizzi, Org. Lett., 4 (2002) 2561-2563.

[37] A. Mirabaud, J. C. Mulatier, A. Martinez, J. P. Dutasta, V. Dufaud, Catal. Today, 281 (2017) 387-391.

[38] B. Chatelet, L. Joucla, J. P. Dutasta, A. Martinez, K. C. Szeto, V. Dufaud, J. Am. Chem. Soc., 135 (2013) 5348-5351.

[39] X. Wang, W. Y. Gao, Z. Niu, L. Wojtas, J. A. Perman, Y. S. Chen, Z. Li, B. Aguila, S. Ma, Chem. Commun., 54 (2018) 1170-1173.

[40] Y. F. Xie, C. Guo, L. Shi, B. H. Peng, N. Liu, Org. Biomol. Chem., 17 (2019) 3497-3506.

[41] G. Bresciani, M. Bortoluzzi, G. Pampaloni, F. Marchetti, Org. Biomol. Chem., 19 (2021) 4152-4161.

[42] C. Phung, D. J. Tantillo, J. E. Hein, A. R. Pinhas, J. Phys. Org. Chem. (2018) 31.

[43] M. Lv, P. Wang, D. Yuan, Y. Yao, ChemCatChem, 9 (2017) 4451-4455.

[44] X. M. Kang, L. H. Yao, Z. H. Jiao, B. Zhao, Chem. Asian J., 14 (2019) 3668-3674.

[45] M. Sengoden, M. North, A. C. Whitwood, ChemSusChem, 12 (2019) 3296-3303.

[46] A. W. Miller, S. T. Nguyen, Org. Lett., 6 (2004) 2301-2304.

[47] A. Zahedi Bialvaei, M. Rahbar, M. Yousefi, M. Asgharzadeh, H. Samadi Kafil, J. Antimicrob. Chemother., 72 (2017) *72*, 354-364.

[48] M. Yan, L. Xu, Y. Wang, J. Wan, T. Liu, W. Liu, Y. Wan, B. Zhang, R. Wang, Q. Li, Drug Dev. Res., 81 (2020) 402-418.

[49] C. Foti, A. Piperno, A. Scala, O. Giuffrè, Molecules, 26 (2021) 4280.

[50] C. Damiano, P. Sonzini, G. Manca, E. Gallo, Eur. J. Org. Chem. (2021) 2807-2814.

[51] P. Sonzini, C. Damiano, D. Intrieri, G. Manca, E. Gallo, Adv. Synth. Catal., 362 (2020) 2961-2969.

[52] C. Maeda, S. Sasaki, K. Takaishi, T. Ema, Catal. Sci. Technol. 8 (2018) 4193-4198.

[53] N. V. Suendo, A. Alni, A. A. Nugroho, Y. Majima, S. Lee, Y. P. Nugraha, H. Uekusa, J. Phys. Chem. A, 124 (2020) 2672–2682.

[54] C. T. Kresge, M. E. Leonowicz, W. J. Roth, J. C. Vartuli, J. S. Beck, Nature, 359 (1992) 710-712.

[55] J. S. Beck, J. C. Vartuli, W. J. Roth, M. E. Leonowicz, C. T. Kresge, K. D. Schmitt, C. T. W. Chu, D. H. Olson, E. W. Sheppard, S. B. McCullen, J. B. Higgins, J. L. Schlenker, J. Am. Chem. Soc., 114 (1992) 10834-10843.

[56] D. Zhao, J. Feng, Q. Huo, N. Melosh, G. H. Fredrickson, B. F. Chmelka, G. D. Stucky, Science, 279 (1998) 548-552.

[57] D. Wöhrle, *J. Porphyrins Phthalocyanines*, 1 (1997) 395-396.

[58] J. He, T. Wu, Z. Zhang, K. Ding, B. Han, Y. Xie, T. Jiang, Z. Liu, Chem. Eur. J., 13 (2007) 6992-6997.

[59] F. Lagarde, H. Srour, N. Berthet, N. Oueslati, B. Bousquet, A. Nunes, A. Martinez, V. Dufaud, J. CO2 Util., 34 (2019) 34-39.

[60] J. B. Sweeney, Chem. Soc. Rev., 31 (2002) 247-258.

[61] W. Clegg, R. W. Harrington, M. North, R. Pasquale, Chem. Eur. J., 16 (2010) 6828-6843.